CCFE
CULHAM CENTRE FOR FUSION ENERGY

UK Atomic Energy Authority

UKAEA-CCFE-PR(21)23

K G McClements, J Young, L Garzotti, O M Jones, C A Michael

Abel inversion of soft X-ray fluctuations associated with fast particle-driven fishbone instabilities in MAST plasmas

Abel inversion of soft X-ray fluctuations associated with fast particle-driven fishbone instabilities in MAST plasmas

K G McClements, J Young, L Garzotti, O M Jones, C A Michael

This is a preprint of a paper submitted for publication in
Plasma Research Express

Abel inversion of soft X-ray fluctuations associated with fast particle-driven fishbone instabilities in MAST plasmas

K.G. McClements[1], J. Young[1,2], L. Garzotti[1], O.M. Jones[1,3], C.A. Michael[4]

[1] Culham Centre for Fusion Energy, UKAEA, Abingdon OX14 3DB, UK
[2] Department of Physics, University of Bath, Bath BA2 7AY, UK
[3] Department of Physics, University of Durham, Durham DH1 3LE, UK
[4] Department of Physics, University of California Los Angeles, Los Angeles, California 90095, USA

Email: Ken.McClements@ukaea.uk

Abstract

A set of soft X-ray cameras provided measurements of high frequency instabilities as well as steady-state emission in the Mega Amp Spherical Tokamak (MAST). It is shown that Abel inversion can be readily applied to fluctuating soft X-ray emission from the MAST midplane associated with fast particle-driven "fishbone" instabilities, characterised by toroidal mode number $n = 1$. Each fishbone burst had an early phase in which high amplitude fluctuating soft X-ray signals from the plasma core were close to being in phase with each other, and there was a region close to the outboard plasma edge in which the fluctuations were relatively weak and in antiphase with those in the core. The major radius of the "phase axis" at which the mode amplitude changed sign R_p was initially outboard of the tokamak magnetic axis at R_0, but moved inboard during the burst, eventually becoming close to R_0, at which time the oscillations were of similar amplitude inboard and outboard of R_p. The fishbone radial structure early in the burst can be understood in part by recognising that the mode is supported by energetic ions with a high average toroidal rotation rate: in a co-rotating frame, the effective magnetic axis is shifted outboard by a distance that is comparable to the difference between the major radii of the phase axis early in the burst and the laboratory frame magnetic axis. It is conjectured that the transition to a mode with $R_p \simeq R_0$ occurred because most of the energetic ions were expelled from the plasma core region where the mode amplitude peaked, so that the instability could no longer be characterised as an energetic particle mode. Abel inversion of fishbone soft X-ray emission thus provides useful insights into the nature of energetic particle modes in tokamak plasmas and their relationship with MHD modes.

1 Introduction

Fishbones are instabilities driven by fast (suprathermal) particles in tokamak plasmas when the safety factor q (defined as the number of toroidal circuits made by an equilibrium magnetic field line in one poloidal circuit) drops to values approaching unity

in the plasma core region [1]. They occurred frequently during neutral beam heating in the Mega Amp Spherical Tokamak (MAST), with beam ions providing the fast particle population needed to drive the instability. A list of typical plasma parameters in MAST, along with a description of the phenomenology and consequences of fishbones in that device, can be found in Ref. [2]. Briefly, MAST plasmas had major and minor radii $R \simeq 0.9\,\mathrm{m}$, $a \simeq 0.6\,\mathrm{m}$, the toroidal magnetic field at the magnetic axis was about $0.4\,\mathrm{T}$, the plasma current was typically in the range 400 - 900 kA, and the primary injection energy of beam ions (deuterons) was usually around 60-70 keV. The fuel ion species in nearly all MAST plasmas was deuterium. Core electron densities and temperatures were up to a few times $10^{19}\,\mathrm{m}^{-3}$ and 1 keV. Fishbone instabilities could be detected using magnetic (Mirnov) coils and several soft X-ray cameras, whose data acquisition rate (several hundred kHz) was high enough to resolve individual fishbone oscillations at the typical initial frequencies of these modes (a few tens of kHz). After the initial excitation of a fishbone, the mode frequency was observed to chirp down rapidly (in about 2-3 ms) to a value close to the toroidal plasma rotation frequency, at which point the mode disappeared. This burst cycle usually repeated several times before a transition to a so-called long-lived mode, believed to be a saturated kink mode in the plasma core.

Much of the interest in fishbones arises from the fact that while they are generally benign in terms of their direct effects on the bulk plasma, they can cause non-classical transport or loss of the fast particles that drive them. For this reason they can frustrate attempts to achieve optimum performance in tokamak plasmas by injecting higher levels of auxiliary heating. In the case of MAST this was demonstrated most clearly in an experiment showing that a doubling of neutral beam power resulted in the neutron yield (which was mainly due to beam-thermal DD fusion reactions) rising by only about 40% rather than the classically-predicted figure of about 100%. This was due to an increase in fast ion redistribution and loss arising from the excitation of fast ion-driven instabilities, including fishbones [3]. It is important therefore to understand as fully as possible the nature of these modes, and our aim in this paper is to to glean information on their spatial structure through a careful examination of soft X-ray data.

The paper is structured as follows. Following a description of soft X-ray and Mirnov coil measurements of fishbones in MAST (Section 2), we demonstrate in Section 3 that spatially-resolved measurements of fishbones obtained using one of the MAST soft X-ray cameras can be Abel-inverted to yield the midplane radial structure of the unstable mode. We show that the radial structure changes during the course of a fishbone burst, and suggest a possible interpretation of this phenomenon in Section 4. A summary is provided in Section 5.

2 Soft X-ray and Mirnov coil measurements of fishbones in MAST

The MAST tangential soft X-ray camera detects optically thin, line-integrated emission along a set of chords that lie approximately in the plasma midplane and can be distinguished by their tangency radius p - the major radius R at which the chord is

tangential to a flux surface, as shown in figure 1. The coordinate labels in this figure will be used later when discussing Abel inversion of soft X-ray fluctuations associated with fishbones.

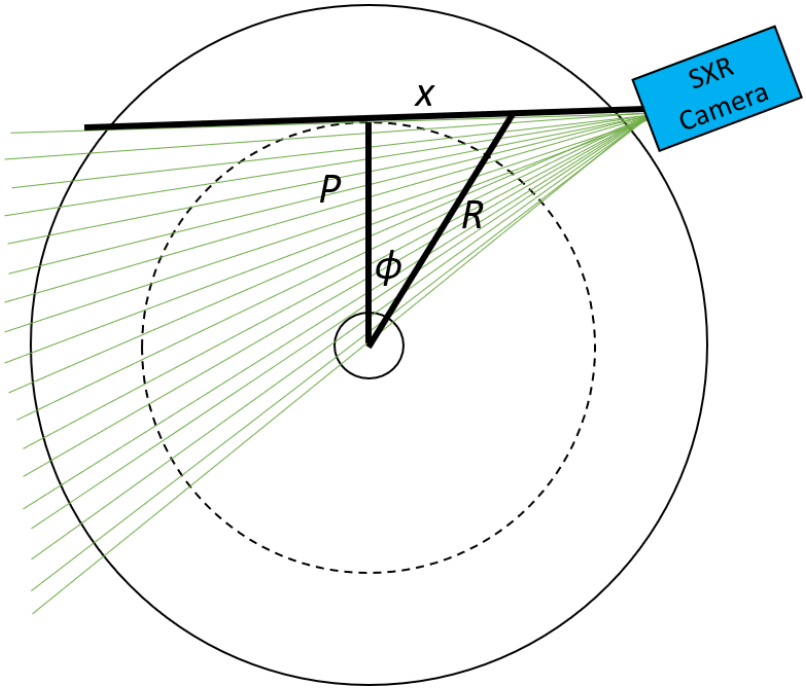

Figure 1: Vertical view of MAST showing layout of tangential soft X-ray camera. The green lines show the camera lines-of-sight, and the coordinate labels used in the text are those indicated here. The dashed circle is the outer plasma boundary, and the two solid curves show the locations of the vacuum vessel and centre post.

The soft X-ray cameras on MAST used beryllium filters with a thickness of 15 μm to block photons with energies below a value $\mathcal{E}_0 \simeq 1\,\mathrm{keV}$. This made it possible to exclude line emission from dominant impurities, in particular carbon. The detected signal is due primarily to thermal bremsstrahlung. Assuming that the plasma is fully ionised, the local emission j from a given volume has the following dependence on electron density n_e, electron temperature T_e and effective ion charge state Z_{eff} [5]:

$$j = J_0 n_e^2 T_e^{1/2} Z_{\mathrm{eff}} e^{-\mathcal{E}_0/T_e}, \tag{1}$$

where J_0 is a constant and we have followed common practice in neglecting the weak dependence of the Maxwellian-averaged Gaunt factor on T_e. The signal is thus sensitive to local fluctuations in n_e, T_e or Z_{eff}. The high magnetic Reynolds numbers characteristic of tokamak plasmas ensure that the magnetic field is frozen into the plasma to a good approximation, and therefore magnetic field perturbations such as those associated with fishbones would be expected to result in local fluctuations in quantities

such as electron temperature and density. It has also been suggested that the temporal evolution of fishbones in MAST could have been affected by rapid changes in Z_{eff} associated with localised accumulation of highly-charged impurity ions [6].

Figure 2 shows time traces of soft X-ray fluctuations on tangential camera chords with tangency radii close to the magnetic axis during the evolution of a fishbone in MAST shot 29976. The amplitude of the fishbone in the magnetic coil trace peaks at approximately 0.2013 s, so the period shown in the figure includes the growth and decay phases of the instability. It should be noted that each panel overlaps with the preceding panel by 3 ms, and that the intensity scaling of each panel is arbitrary. The soft X-ray detectors are uncalibrated, but the instrument response is reasonably uniform across channels.

We can draw two important conclusions from figure 2. First, at late times (after about 0.2013 s) there is a clear antiphase relationship between fluctuations in channels with p greater than about 0.8 m and those with tangency radii below this value. In this phase of the fishbone burst the time interval between intensity maxima in any given channel corresponds to a frequency of about 25 kHz, which is close to the frequency of the fishbone itself at this stage. This behaviour is characteristic of an instability with dominant toroidal mode number $n = 1$, and indeed signals from toroidally-distributed Mirnov coils at this time confirm that this is the case. The second conclusion we can draw from figure 2 is that during the early part of the burst the signals corresponding to essentially all of the channels with p less than about 1.0 m are in phase with each other, or very nearly so. The change during the course of a fishbone burst in the phase relationship between fluctuations corresponding to different lines-of-sight apparent in figure 2 occurs frequently in MAST. It is not clear how to interpret this result in terms of local plasma parameters, however, since the fluctuating intensities in figure 2 are line-integrated. In the following section we will show how local fluctuations in soft X-ray intensity can be inferred from soft X-ray camera data using Abel inversion.

3 Abel inversion of soft X-ray measurements

3.1 Analysis

In the case of axisymmetric soft X-ray emission we can write

$$I(p) = \int_{-x_{\text{edge}}}^{x_{\text{edge}}} j(x)dx, \tag{2}$$

where j is the local soft X-ray emissivity, x is distance along a chord relative to the point at which the chord is tangential to a flux surface (where $p = R$), and $\pm x_{\text{edge}}$ are the values of x where the chord enters and leaves the plasma (see figure 1). Transforming the integration variable from x to R it is evident that Eq. (2) becomes

$$I(p) = 2\int_{p}^{R_{\text{out}}} \frac{j(R)R}{\sqrt{R^2 - p^2}}dR, \tag{3}$$

where R_{out} is the major radius of the outer plasma boundary in the midplane. The measured soft X-ray intensity is thus the Abel transform of the local emissivity, j [5, 7].

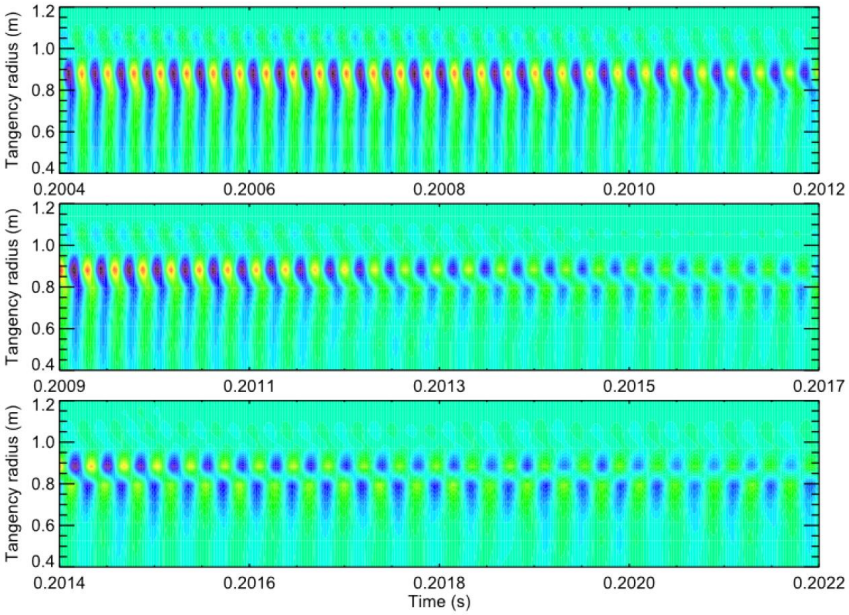

Figure 2: Fluctuations in 20-40 kHz bandpass-filtered soft X-ray signal during fishbone in MAST pulse 29976. The tangengy radius is identical to the parameter p in figure 1.

An analytical formula exists for the inverse Abel transform, making it possible for $j(R)$ to be inferred from $I(p)$. The challenge we have is that the fluctuating j associated with fishbones has toroidal mode number $n = 1$, as discussed in the previous section, and therefore we cannot simply replace j in Eq. (3) with the fluctuating intensity and evaluate the inverse transform. Although fishbone frequencies typically chirp down rapidly, at any given instant the spectrum is usually strongly-peaked at a well-defined mode frequency ω. This can be seen in figure 3 for the case of the fishbone plotted in figure 2. The perturbation to j resulting from a fishbone propagating in the positive φ direction (in MAST this was the plasma current direction) with $n = 1$ can thus be represented by an expression of the form

$$j_1(R, \varphi, t) = j_0(R) \cos(\varphi - \omega t), \tag{4}$$

where j_0 is the function we aim to determine. The corresponding perturbation to I is denoted by I_1. It is evident from figure 1 that $\cos\varphi = p/R$, and so I_1 is not the Abel transform of j_1. A further complication is that while φ can be defined as toroidal angle as shown in figure 1, this implies a different definition of φ for each line-of-sight since these are not parallel but form a fan, converging on the camera itself. For definiteness, we define φ such that $\cos\varphi = p/R$ for the outermost tangential soft X-ray camera chord, with tangency radius $p \equiv p_1$. For every other chord $\cos(\varphi - \varphi_{pi}) = p_i/R$ where φ_{pi} is a constant for the i-th chord with tangency radius $p = p_i$: it is the angle made by the i-th chord relative to the outermost chord at the pinhole camera, which is also the angle made by the line joining the tangency point to the tokamak symmetry axis with respect to the corresponding line for the outermost chord.

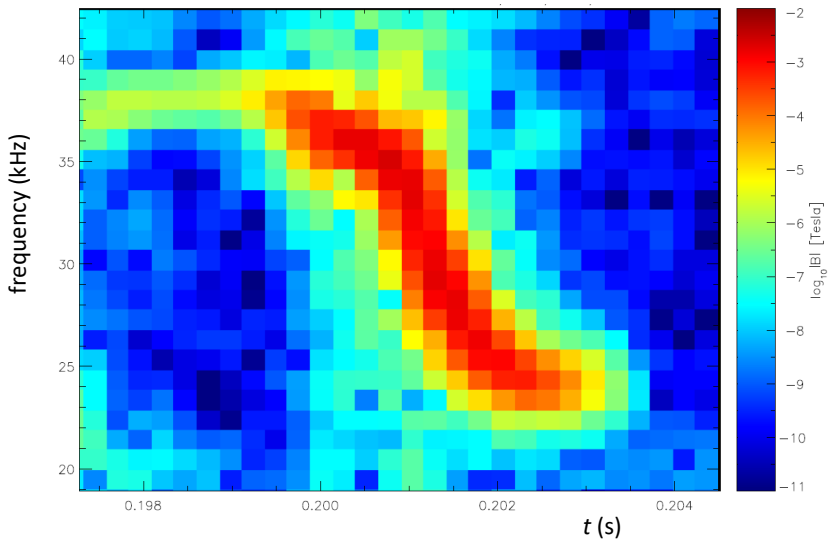

Figure 3: Spectrogram of Mirnov coil fluctuations for the fishbone shown in figure 2. A fast Fourier transform was used to generate this plot, with a Hann window function [4] of duration 1.02 ms and overlap 75%.

Abel inversion can now be applied to this problem as follows. Empirically, on timescales shorter than that of the fishbone chirp, the perturbation to I can be described as having a time variation characterised by a single frequency, ω:

$$I_1(p,t) = I_0(p)\cos(\omega t). \tag{5}$$

Multiplying this expression by $\cos(\omega t - \varphi_{pi})$ and taking the time-average of the resulting equation over one wave cycle, we obtain

$$\langle I_1(p,t)\cos(\omega t - \varphi_{pi})\rangle = \frac{1}{2} I_0(p)\cos\varphi_{pi}, \tag{6}$$

where the angled brackets denote a time average. Similarly, multiplying j_1 by $\cos(\omega t - \varphi_{pi})$, taking the time-average over one wave cycle and dropping the subscript i on p_i yields

$$\langle j_1(R,\varphi,t)\cos(\omega t - \varphi_{pi})\rangle = \frac{1}{2} j_0(R)\cos(\varphi - \varphi_{pi}) = \frac{p}{2R} j_0(R). \tag{7}$$

Since I_1 and j_1 satisfy Eq. (3), we infer from Eqs. (6) and (7) that I_0 and j_0 satisfy

$$I_0(p)\cos\varphi_{pi} = 2\int_p^{R_{\text{out}}} \frac{j_0(R)p}{\sqrt{R^2 - p^2}} dR. \tag{8}$$

This can be rearranged to give

$$\frac{I_0(p)\cos\varphi_{pi}}{p} = 2\int_p^{R_{\text{out}}} \frac{[j_0(R)/R]R}{\sqrt{R^2 - p^2}} dR. \tag{9}$$

Thus $I_0 \cos\varphi_{pi}/p$ is the Abel transform of j_0/R, and we can therefore express j_0 in terms of I_0 using the inverse transform [5]:

$$j_0(R) = -\frac{R}{\pi}\int_R^{R_{\rm out}} \frac{d}{dp}\left(\frac{I_0\cos\varphi_{pi}}{p}\right)\frac{dp}{\sqrt{p^2-R^2}}. \qquad (10)$$

It should be noted here that φ_{pi} is a constant for each tangential soft X-ray camera line-of-sight. From its definition [Eq. (5)], it can be seen that I_0 is simply the peak amplitude of the measured soft X-ray intensity in one wave cycle. Equation (10) provides an exact inversion of the measured intensity. It should be noted however that the inversion requires I_0/p to be differentiated. In the case of real experimental data, this operation must of course be carried out numerically, and numerical differentiation of noisy data tends to amplify the effects of the noise. It is important therefore to reduce data noise as much as possible. This can be achieved using digital demodulation, discussed in the next subsection.

The integration in equation (10) must be performed using the trapezoidal rule with a fixed number of points in dummy variable space since the integrand can only be evaluated at values of this variable corresponding to the geometry of the tangential soft X-ray camera. Moreover the intervals between successive p values are not exactly constant. A further complication is that difficulties typically arise from the singularity in the integrand at $p = R$. This difficulty can be eliminated however by transforming the dummy integration variable to $q = \sqrt{p^2 - R^2}$. The intervals between successive q values in the integral are also, of course, non-uniform.

3.2 Digital demodulation of soft X-ray data

A description of the method of of digital demodulation can be found for example in Ref. [8]. This entails the removal of the carrier frequency ω from a fluctuating signal so that it becomes steady over time intervals that are short compared to the timescale on which ω itself changes (in the present case, the timescale of a fishbone burst: typically 2-3 ms) but much longer than the period of a single oscillation (a few tens of microseconds). Signals can thus be aggregated over relatively long periods, reducing photon shot noise and hence making it more viable to use the Abel inversion expression, Eq. (10).

A further correction must be applied to take into account the systematic phase shift apparent between different soft X-ray channels in figure 2 at late times in the fishbone burst. These shifts are considerably larger than those arising from the fan geometry of the lines of sight shown in figure 1. The phase difference can be obtained by using any chosen soft X-ray or Mirnov coil signal as a reference and determing the phase of any other soft X-ray channel relative to this. The two frames of figure 4 show the result of applying this to the demodulation of fluctuations recorded in two neighbouring tangential channels when the reference phase was obtained using a Mirnov coil signal. For channel 11, the soft X-ray signal remains in phase with the coil signal throughout the fishbone. For channel 12, on the other hand, at slightly higher p, the two signals are in phase early in the burst but are in antiphase by the end of the burst, reflecting the transition in mode structure shown in figure 2. It is important to stress here that

the choice of reference signal is arbitrary provided that the phase relationship between fluctuations in different soft X-ray lines-of-sight is correctly captured.

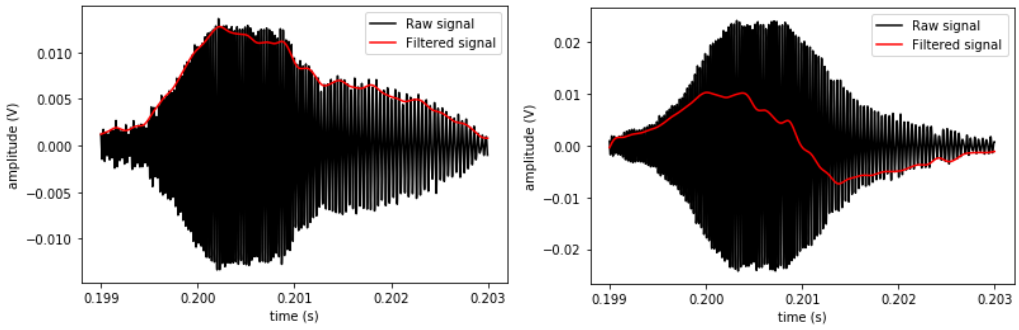

Figure 4: Raw (black curves) and filtered (red curves) signals for fishbone in MAST pulse 29976 recorded using tangential soft X-ray camera channel 11 (left) and channel 12 (right).

3.3 Results

Figure 5 shows the results of Abel inversion (with digital demodulation) applied to fluctuating soft X-ray data from the fishbone burst shown in figure 2. As discussed in section 2, the soft X-ray detectors are uncalibrated, and small differences in the instrument response across different lines-of-sight will of course propagate into Abel-inverted mode amplitudes. Moreover, as discussed previously, the Abel inversion itself introduces numerical errors, and the use of a Mirnov coil signal to provide a reference phase entails an additional small experimental error. The radial profile at any instant shown in figure 5 should therefore not be regarded as a fully accurate representation of the fishbone eigenfunction. We can nevertheless draw some useful inferences from this figure (we will comment later on the cumulative effects of the experimental and numerical errors in the Abel inversion process).

With large phase shifts relative to an arbitrarily-chosen reference signal taken into account, it is possible for the demodulated amplitude to be of either sign. As in the case of figure 2, it is more instructive to discuss the late phase of the burst first ($t > 0.201\,\mathrm{s}$), since the mode structure in this phase is easier to interpret. During this period the mode has a very simple structure, with positive amplitude inboard of $R \simeq 0.9\,\mathrm{m}$ and negative amplitude (of similar magnitude) at higher major radii. It is possible to define a "phase axis" $R = R_p$ where the amplitude changes sign: during the late phase of this fishbone $R_p \simeq 0.9\,\mathrm{m}$. A reconstruction of the plasma equilibrium at this time using the EFIT code [9] indicates that this value of R_p is consistent with the major radius of the magnetic axis, within experimental uncertainties arising mainly from the fact that the soft X-ray lines-of-sight have a finite separation from each other (the p values for channels 11 and 12, for example, differ by about 9 cm).

Early in the burst, on the other hand, the mode amplitude is of the same sign across

the entire plasma core region, extending from about 0.6 m to 1.04 m: the choice of reference signal is such that the amplitude in this region plotted in figure 5 happens to be positive. Outboard of 1.04 m the amplitude is weakly negative, and thus during this period there is a phase axis at this major radius.

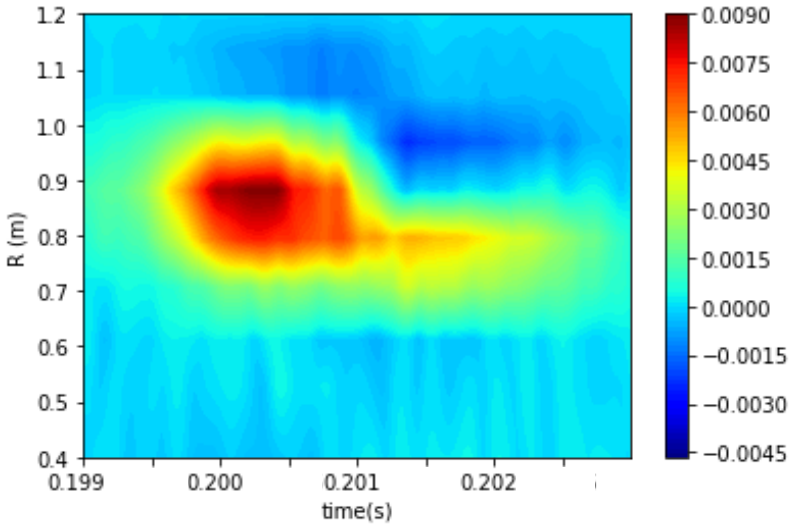

Figure 5: Amplitude of soft X-ray fluctuations versus major radius R and time during a fishbone in MAST pulse number 29976, calculated using Abel inversion of measured soft X-ray emission in the plasma midplane.

To obtain a more complete picture of the mode structure, it is useful to examine also the fluctuating soft X-ray emission detected using the upper and lower horizontal cameras. These provide poloidal views of the plasma respectively below and above the midplane at a fixed toroidal angle. Due to the non-circularity of flux surfaces in MAST plasmas, Abel inversion of the emission is not possible in this case. However the non-inverted fluctuation data can still be demodulated and plotted in the tangency radius - time plane, as shown in figure 6 for the fishbone plotted in figures 2 - 5. In this case negative values of p correspond to lines-of-sight below the midplane. While it is apparent from figure 6 that the intensity of the fluctuations varies during the burst, peaking at about 0.201 s, it is evident that the essential spatial (vertical) structure of the mode doesn't change, in contrast to the change in radial structure shown in figures 2 and 5. A simple antiphase relationship is apparent between the mode amplitudes on each side of the midplane line-of-sight ($p = 0$) throughout the burst, consistent with the burst having a dominant poloidal mode number $m = 1$.

The mode evolution apparent in figures 2-6 is qualitatively similar to that seen in many other fishbones occurring in MAST, and thus appears to be generic. In many of the events studied we find that during the early phase of a fishbone the associated soft X-ray fluctuations around the plasma core region are in phase with each other, and a reversal is observed in the sign of the amplitude at a major radius lying well outboard of the tokamak magnetic axis, by up to about 15 cm in some cases. In the

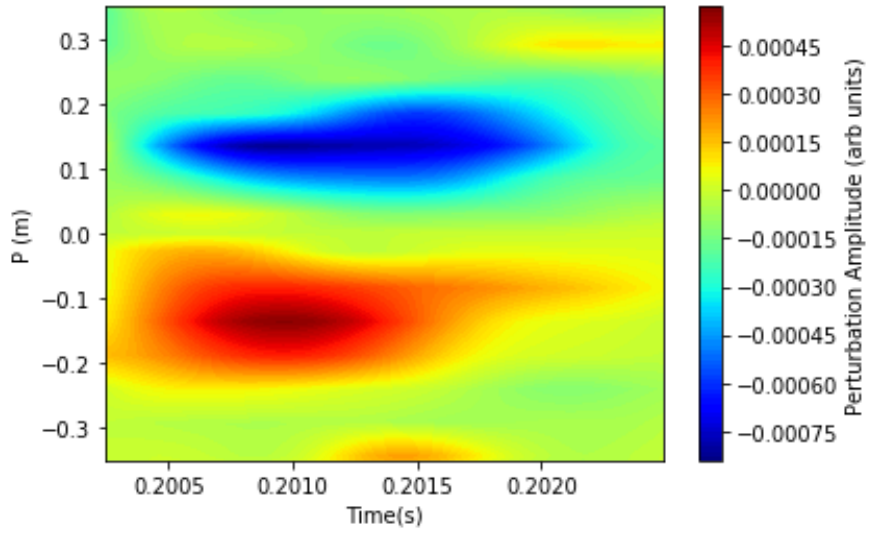

Figure 6: Demodulated soft X-ray emission due to first fishbone in MAST pulse 29976 obtained using the upper and lower horizontal cameras ($p < 0$ corresponds to the region below the midplane). The dominant poloidal mode number is $m = 1$ as expected.

late phase of each fishbone there is a transition in the radial mode structure, with the phase axis moving inboard to a major radius close to that of the magnetic axis. The fact that this transition in mode structure is observed in many different fishbones, combined with the evidence for a transition in the raw soft X-ray data (figure 2), provides a strong indication that it cannot be attributed to random errors, associated for example with photon shot noise. Systematic errors in the data are also present but, as discussed earlier, the soft X-ray instrument response is fairly uniform across channels, and therefore the conclusions presented here are unlikely to be explicable in terms of any such errors.

4 Interpretation of radial mode structure

As discussed above, the results plotted in figure 6 suggest strongly that the dominant poloidal mode number of fishbones in MAST is $m = 1$, as expected for an instability of this type. In the case of an $m = n = 1$ magnetohydrodynamic (MHD) eigenfunction, plotted as a function of R in the midplane, we would expect to observe a null at the magnetic axis, since at this point there is a shift of π in the poloidal angle. This is indeed what we observe late in the burst, when the phase and magnetic axes are coincident to within the spatial resolution provided by the tangential soft X-ray camera. However, the observations that the fluctuating signals in core tangential soft X-ray channels are close to being in phase with each other (figure 2), and the presence of a large outboard shift of the phase axis early in each burst (figure 5), do *not* appear to be compatible with MHD and require an explanation.

In seeking a possible explanation, we first note that fishbones have often been char-

acterised as energetic particle modes rather than MHD modes [10]. This means that in addition to being driven unstable by energetic particles, the mode eigenfunctions themselves are determined primarily by the properties of the energetic particle population rather than those of the thermal plasma. Nevertheless the fact that they are detected as magnetic fluctuations indicates that they can still be regarded as eigenmodes of the equilibrium field. That being the case, it is worth considering what this field looks like from the perspective of the beam ions that are driving the modes. In the pulses considered in this paper the beams were injected in the co-current direction, and the steady-state beam ion distribution was strongly weighted towards that direction since significant pitch angle scattering only occurred in the latter stages of the collisional slowing-down process. This means that the beam ion population had a large mean toroidal velocity, and it is appropriate to consider a reference frame that is co-rotating with those ions. In this frame charged particles are subject to centrifugal and Coriolis forces in addition to the Lorentz force, and both the Coriolis and Lorentz forces are proportional to the cross product of a vector with the particle velocity. The immediate consequence of this is that the rotation rate of the frame Ω causes the effective magnetic field $\mathbf{B}_*$ to differ from the laboratory frame field $\mathbf{B}$ as follows [11]:

$$\mathbf{B}_* = \mathbf{B} + \frac{2m}{e}\Omega\hat{\mathbf{Z}}, \tag{11}$$

where m, e are the beam ion mass and charge while $\hat{\mathbf{Z}}$ is the unit vector in the positive (upward) vertical direction. Since the plasma current (and hence the beam rotation) direction in MAST was anti-clockwise as seen from above, it follows that Ω in Eq. (11) should be taken to be numerically positive. Since the rotation vector is vertical, it affects only the poloidal magnetic field. A plasma current that is anti-clockwise in the horizontal plane (as viewed from above) generates a poloidal field that is clockwise in the (R, Z) plane, and therefore the rotation term in Eq. (11) is oppositely directed to the vertical field outboard of the magnetic axis and in the same direction as B_Z on the inboard side. This has the effect of moving the flux surfaces to higher R, as shown in figure 4c of Ref. [12].

The location of the effective magnetic axis is also moved outboard, and it is straightforward to quantify this shift from Eq. (11). Fishbone excitation indicates that $q \simeq 1$ in the core region of MAST, which can be approximated as a large aspect tokamak plasma and therefore it is acceptable to use the cylindrical expression [13]

$$q = \frac{r}{R_0}\frac{B_0}{B_\theta}, \tag{12}$$

where B_θ is the poloidal field at distance r from the magnetic axis where the toroidal field is equal to B_0. It follows from Eq. (12) that

$$B_\theta = \frac{rB_0}{R_0 q} \simeq \frac{rB_0}{R_0}, \tag{13}$$

where we have used $q \simeq 1$. In the outer midplane $B_\theta = B_Z$ and is numerically negative. It can therefore cancel the rotation term in Eq. (11), giving an effective poloidal field

null in the rotating frame at a major radius given by

$$R = R_0 + \frac{2mR_0\Omega}{eB_0} = \left(1 + 2\frac{\Omega}{\Omega_i}\right) R_0, \tag{14}$$

where Ω_i is the beam ion cyclotron frequency corresponding to the magnetic field B_0. To evaluate the outboard shift in the effective magnetic axis position we need to determine an appropriate value for the mean rotation rate associated with the beam ions, Ω. A typical example of a steady-state beam ion distribution in the core region of a high performance MAST plasma is shown in the left hand frame of figure 10 in [14]. This distribution, calculated using the NUBEAM module of the TRANSP code, is strongly anisotropic, peaking at a pitch close to -1 (the negative sign is due to the fact that plasma current and toroidal field in MAST were oppositely-directed), and the peak energy is about 15 keV. The toroidal deuteron speed v_φ corresponding to this is around $10^6\,\mathrm{ms}^{-1}$, while the toroidal rotation rate is $\Omega = v_\varphi/R_0 \simeq 10^6\,\mathrm{rad\ s}^{-1}$. Using an appropriate toroidal field (0.4 T) to evaluate Ω_i, we infer from these figures and equation (14) an outboard shift in the effective magnetic axis location of about 10 cm, which is close to the phase axis shift in the early period of the fishbone whose radial structure is shown in figure 4. We propose that the phase axis during this stage of the burst coincides with the effective magnetic axis of the plasma in a frame that is co-rotating with the fast ions driving the instability. The incompatibility of our Abel inversion results with MHD, noted at the beginning of this section, can thus be resolved by recognizing that early-stage fishbones are energetic particle modes whose radial structure is determined in part by the effective magnetic field in a frame that is co-rotating with the energetic particles. This interpretation does not by itself provide an explanation for the full radial structure of the early-stage fishbone, in particular the fact that its absolute amplitude is higher on the inboard side of the phase axis than it is on the outboard side. This asymmetry may be a consequence of the fact that fast ion distributions in double null MAST pulses such as this one were generally very strongly peaked in the plasma core region (see figures 7 and 8 in Ref. [3]).

It remains to be explained why the radial structure of the mode transitions to one that *does* appear to be broadly compatible with MHD, i.e. that is characterised by a phase axis lying close to the magnetic axis in the laboratory frame. It seems likely that this can be attributed to the fishbone-induced expulsion of fast ions from the plasma core region noted in Section 1. Direct evidence for the expulsion of fast ions during fishbones in MAST is provided by drops in both volume-integrated neutron count rates (measured using a fission chamber) and fast ion deuterium-alpha (FIDA) emission from the plasma core [2]. The neutron rate is a useful proxy for the fast ion content of the plasma since most fusion reactions in MAST occur between beam ions and thermal ions. The total neutron rate tends to be reduced by the expulsion of fast ions from the core region, first because the thermal ion density is generally lower in the plasma periphery than in the core, and second because many of the fast ions ejected from the core are subsequently lost promptly from the plasma due to finite orbit width and Larmor radius effects. Figure 7 shows the temporal variation of neutron rate during the fishbone studied in this paper. While there is little change in the total neutron rate over the entire time window, it is substantially lower on average

during the late phase of the fishbone ($\sim 201 - 202\,\mathrm{ms}$) than it is in the early phase ($\sim 200 - 201\,\mathrm{ms}$). This is consistent with a depletion of fast ions in the plasma core during the course of the fishbone burst. Spatially-resolved neutron measurements in earlier pulses provide further evidence for fishbones (together with other fast particle-driven modes) depleting the fast ion population in MAST plasmas [3]. It may be expected that a fishbone eigenfunction will transition to an MHD mode if fast ions capable of resonating with the mode, in particular, are expelled. Resonance in this context means that a linear combination of the characteristic toroidal and poloidal frequencies of the fast ions' orbital motion is close to the mode frequency: it is these fast ions that both drive the fishbone and are most susceptible to being transported by it [15].

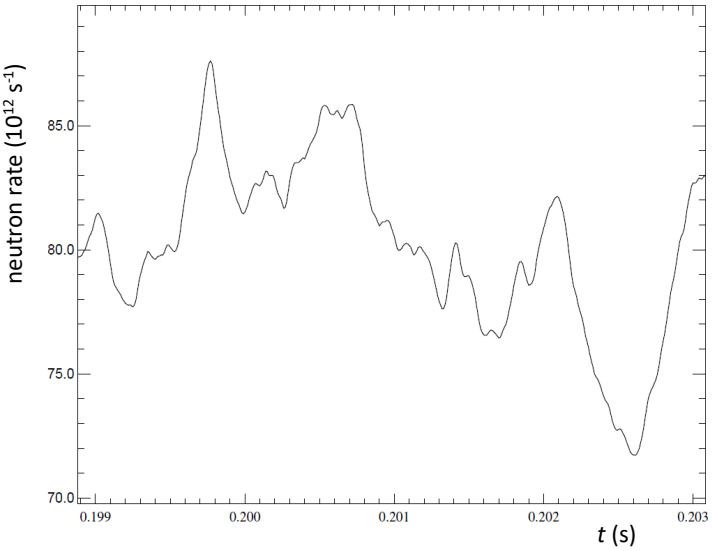

Figure 7: Temporal variation of volume-integrated neutron rate measured using the MAST fission chamber during the fishbone shown in figures 2-6.

As discussed above, fishbones are generally assumed to be internal kink modes with $m = n = 1$, and in such cases a resonant MHD instability can only occur if $q < 1$ somewhere in the plasma [13], although not necessarily at the magnetic axis. Jones and co-workers carried out a careful equilibrium analysis of a MAST pulse during a period of fishbone activity, taking into account motional Stark effect measurements of the magnetic field pitch [2]. This yielded a best-fit q-profile which dropped below unity only towards the end of the period of fishbone activity, and even then only very slightly, by an amount that was within experimental uncertainties. This raises a problem since, although it has always been recognized that fast particle drive is necessary for fishbone excitation, the existence of a $q = 1$ surface in the plasma is also normally assumed to be a prerequisite [1].

Again, transforming to a frame that is co-rotating with the fast ions may help to resolve this problem. In the cylindrical limit the on-axis safety factor q_0 can be written

as [13]

$$q_0 = \frac{2B_0}{\mu_0 j_0 R_0}, \tag{15}$$

where μ_0 is free space permeability and j_0 is the plasma current density at the axis. The effective vertical field associated with the rotation term in Eq. (11) has no effect on the effective current density, since it is a constant and therefore curl-free, and the current profile in the core region of MAST is generally fairly broad. However, as we have demonstrated above, transforming to a frame that is co-rotating with the beam ions produces an increase in the major radius of the effective magnetic axis, i.e. the radius at which the poloidal component of $\mathbf{B}_*$ vanishes. Moreover, while the toroidal field is unaffected by the frame transformation, the value of B_0 that should be used in Eq. (15) will drop since this field component varies approximately as $1/R$. Thus, a 10% increase in the effective magnetic axis radius (comparable to that estimated above) implies a 20% drop in the effective value of q in the plasma core, potentially causing it to fall well below unity. The combination of fast particle drive and, effectively, $q < 1$ might then satisfy the requirements for instability. This interpretation suggests that fishbones are unlikely to be excited by isotropic fast ions (for example fusion alpha-particles in a thermonuclear tokamak reactor) provided that q in the laboratory frame is maintained above unity, since this is also the mean rest frame of the fast ions. However it should be noted that we have not considered the response of the bulk plasma, which flows supersonically in a frame that is co-rotating with the fast ions, and therefore further analysis would be required to establish a more rigorous basis for this conjecture.

5 Summary

We have demonstrated that the midplane radial structure of fast particle-driven bursting fishbone instabilities in MAST can be obtained through Abel inversion of fluctuating soft X-ray signals. Each burst has an early phase in which high amplitude fluctuating soft X-ray signals from the plasma core are close to being in phase with each other, and there is a region close to the outboard plasma edge in which the fluctuations are relatively weak and in antiphase with those in the core. The major radius of the phase axis at which the mode amplitude changes sign R_p is initially outboard of the tokamak magnetic axis at R_0, but it moves inboard during the burst, eventually becoming close to R_0.

The fishbone radial structure early in the burst can be understood in part by recognising that the mode is supported by energetic ions with a high average toroidal rotation rate: in a co-rotating frame, the effective magnetic axis is shifted outboard by a distance that is comparable to the difference between the major radii of the phase axis early in the burst and the true (laboratory frame) magnetic axis. We conjecture that the transition to a mode with $R_p \simeq R_0$ occurs because most of the energetic ions are expelled from the plasma core region where the mode amplitude peaks, so that the instability can no longer be characterised as an energetic particle mode. Abel inversion of soft X-ray emission associated with fishbones in MAST thus provides useful insights into the nature of energetic particle modes in tokamak plasmas and their relationship

with MHD modes.

Acknowledgments

The authors are grateful to Neal Crocker and Henry Wong (both University of California Los Angeles) for helpful conversations. This work was funded partly by the RCUK Energy Programme [grant number EP/T012250/1]. It was also carried out partly within the framework of the EUROfusion Consortium and has received funding from the Euratom research and training programme 2014-2018 and 2019-2020 under grant agreement number 633053. The views and opinions expressed herein do not necessarily reflect those of the European Commission. To obtain further information on the data and models underlying this paper please contact PublicationsManager@ukaea.uk.

References

[1] Chen L, White R B and Rosenbluth M N 1984 *Phys. Rev. Lett.* **52** 1122

[2] Jones O M, Michael C A, McClements K G, Conway N J, Crowley B, Akers R J, Lake R J, Pinches S D and the MAST team 2013 *Plasma Phys. Control. Fusion* **55** 085009

[3] Turnyanskiy M, Challis C D, Akers R J, Cecconello M, Keeling D L, Kirk A, Lake R, Pinches S D, Sangaroon S and Wodniak I 2013 *Nucl. Fusion* **53** 053016

[4] von Hann J 1903 *Handbook of Climatology* (London: McMillan)

[5] Hutchinson I H 1987 *Principles of Plasma Diagnostics* (Cambridge: Cambridge University Press)

[6] Cecconello M, Jones O M, Garzotti L, McClements K G, Carr M, Henderson S S, Sharapov S E, Klimek I and the MAST Team 2015 *Nucl. Fusion* **55** 032002

[7] Nagayama Y, Tsuji S, Kawahata K, Noda N and Tanahashi S 1981 *Japanese Journal of Applied Physics* **20** L779

[8] Powers E J, Don H S, Hong J Y, Kim Y C, Hallock G A and Hickok R L 1988 *Rev. Sci. Instrum.* **59** 1757

[9] Lao L L, St John H, Stambaugh R D, Kellman A G and Pfeiffer W 1985 *Nucl. Fusion* **25** 1611

[10] Hao B, White R, Gao X, Meng G, Li G, Wu B, Wang J, Xu L, Yuan Y, Wei S and EAST Team 2019 *Nucl. Fusion* **59** 076040

[11] Thyagaraja A and McClements K G 2009 *Phys. Plasmas* **16** 092506

[12] McClements K G and McKay R J 2009 *Plasma Phys. Control. Fusion* **51** 115009

[13] Wesson J 2004 *Tokamaks*, 3rd edition (Oxford: Clarendon Press)

[14] Jackson A R, Jacobsen A S, McClements K G, Michael C A and Cecconello M 2020 *Nucl. Fusion* **60** 126035

[15] Lake R 2013 *Consequences of Fast Ion Driven Modes in MAST* (Ph.D. thesis, University of Warwick, `http://wrap.warwick.ac.uk/58299/1/WRAP_THESIS_Lake_2013.pdf`)